NSF IceCube Neutrino Observatory 성균관대학교 SUNGKYUN KWAN UNIVERSITY WIPAC

In-Situ Afterpulse Modeling in IceCube

Taeyun Kim and Chang Dong Rho
for the IceCube Collaboration

Sep. 1, 2026

From Detector Response to Astrophysical Sources

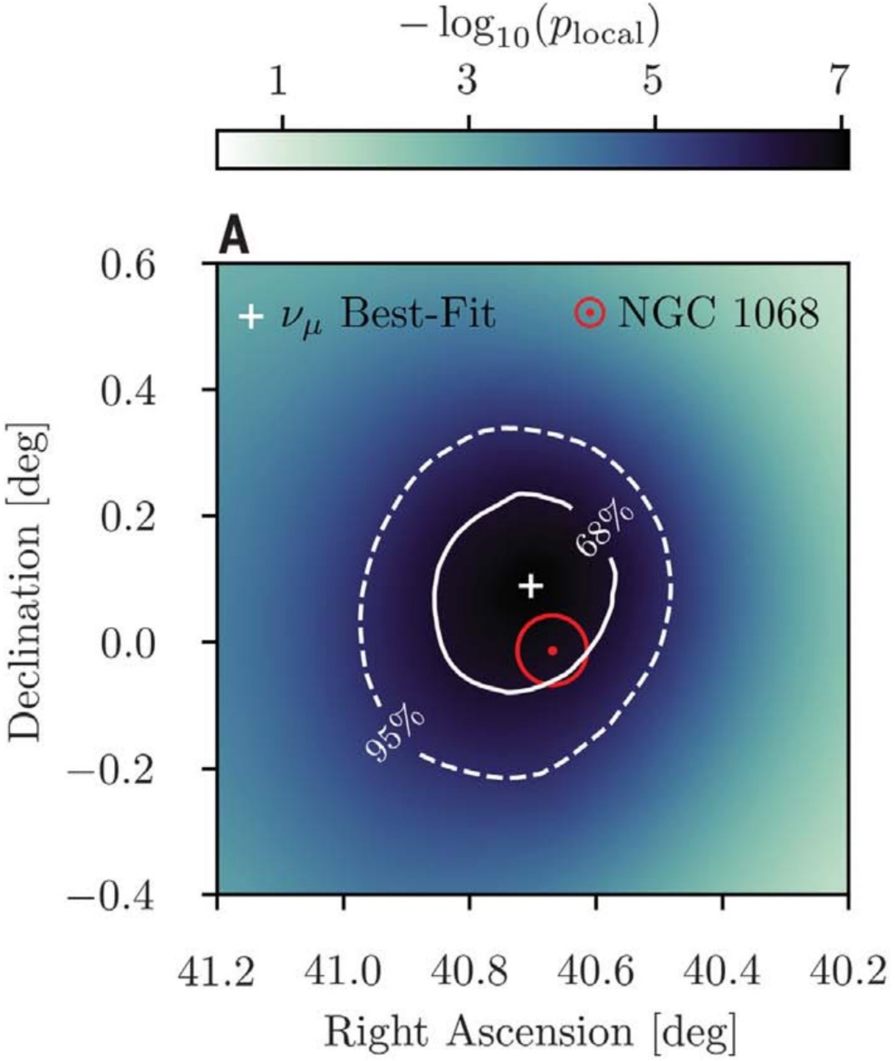

IceCube Collaboration, Science 378 (2022) 538

- Neutrino sources are found by combining many candidate events in a likelihood, each weighted by its own angular uncertainty
- A small, well-modeled angular uncertainty makes a source stand out from the background
- The angular uncertainty, the noise rejection, and the event selection are all derived from detector simulation
- That simulation starts from the detector response
- For IceCube, the detector is the photomultiplier tube (PMT): the pulses it records, with their times and charges

How a Track Direction Is Reconstructed

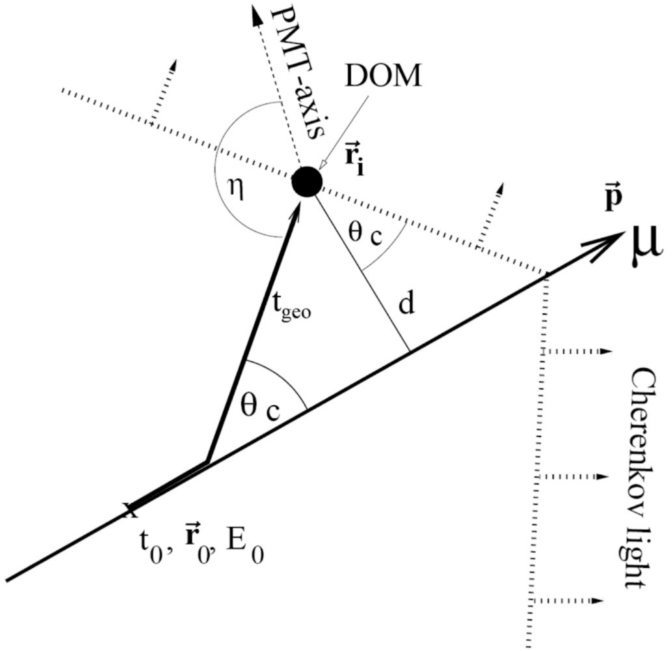

Ahrens et al., NIM A 524 (2004) 169–194.

- t_{geo}: geometric expectation of Cherenkov photon arrival time
- t_{hit}: measured first-PE time

$$L(\Theta) = \prod_{i=1}^{N_{\text{DOMs}}} p^1_{N_i}(t_{\text{res},\,i} \,|\, \Theta), \qquad t_{\text{res}} = t_{\text{hit}} - t_{\text{geo}}$$

- $p^1_N(t_{\text{res}})$: likelihood that the first of N PEs arrives at t_{res}

$$p^1_N(t_{\text{res}}) = N p_1(t_{\text{res}})[S_1(t_{\text{res}})]^{N-1}$$

$$S_1(t_{\text{res}}) = \int_{t_{\text{res}}}^{\infty} p_1(t)dt$$

- Track direction is inferred by maximizing L(Θ) over all DOM hits, using **the arrival time** and **the number of photoelectrons (PEs)** per digital optical module (DOM)

Why Afterpulses Matter for Reconstruction

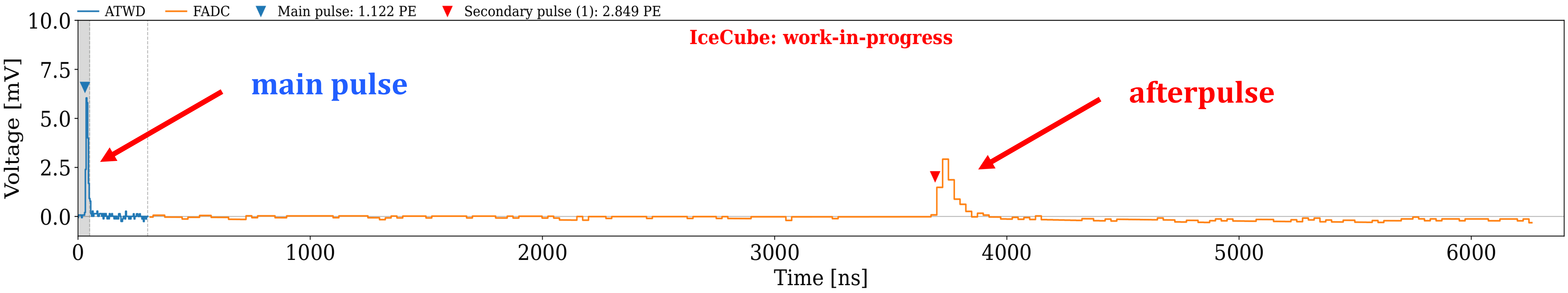

- Afterpulse
  - a pulse that arrives after the main one

Why Afterpulses Matter for Reconstruction

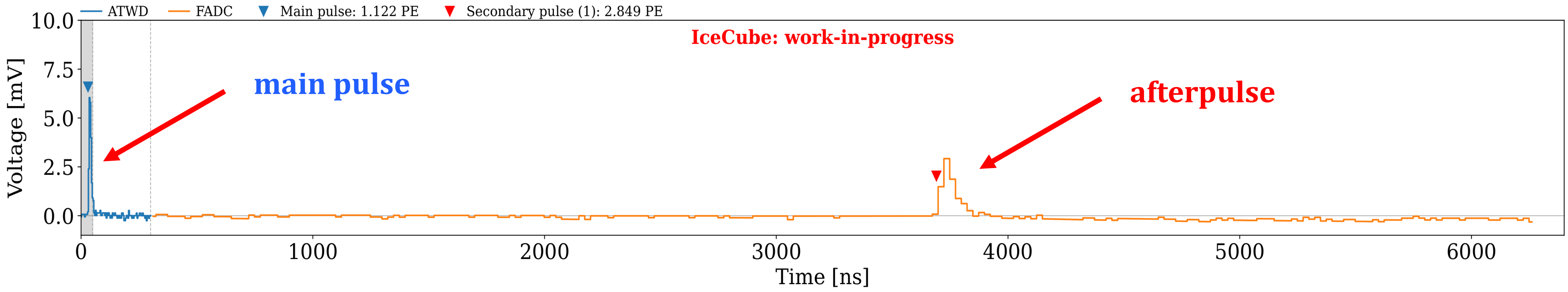

- Afterpulse
  - a pulse that arrives after the main one
  - caused by ionized residual gas molecules inside the PMT that are accelerated back to the photocathode
  - adding pulses to the same DOM, inflating the number of pulses the reconstruction uses
  - an afterpulse can, in turn, make afterpulses of its own

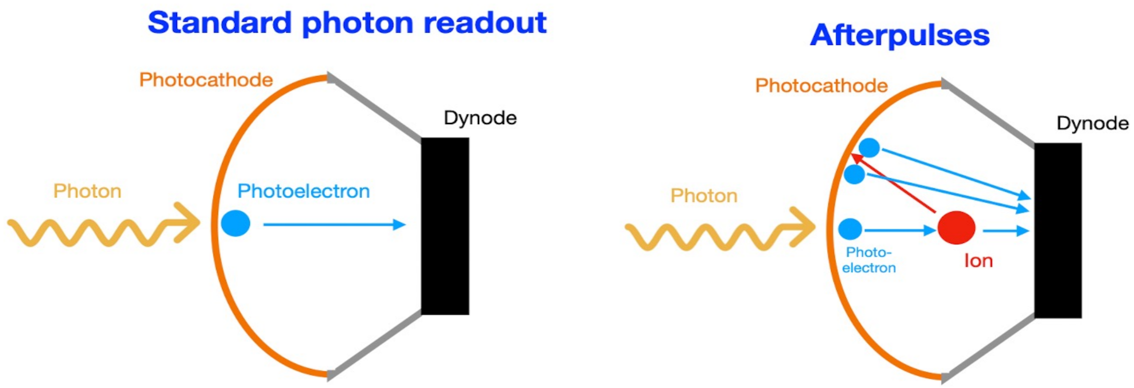

image credit: **Tom Stuttard**

Why Afterpulses Matter for Reconstruction

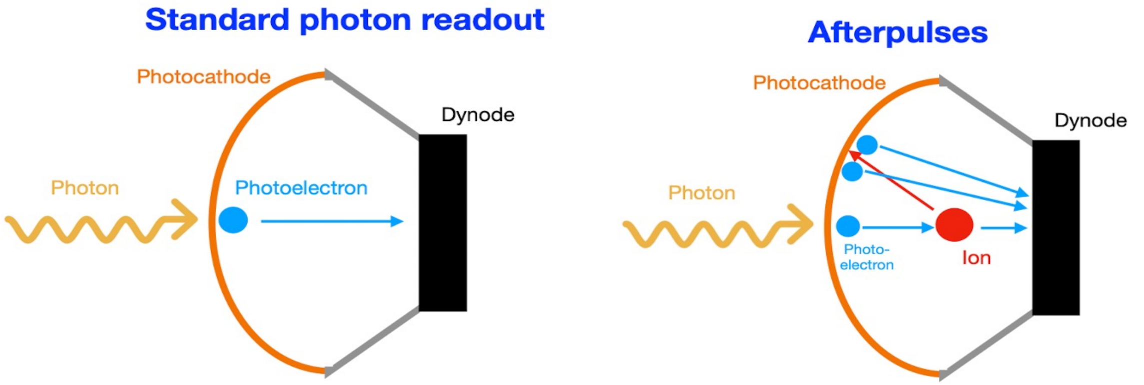

image credit: **Tom Stuttard**

- Afterpulse
  - a pulse that arrives after the main one
  - caused by ionized residual gas molecules inside the PMT that are accelerated back to the photocathode
  - adding pulses to the same DOM, inflating the number of pulses the reconstruction uses
  - an afterpulse can, in turn, make afterpulses of its own

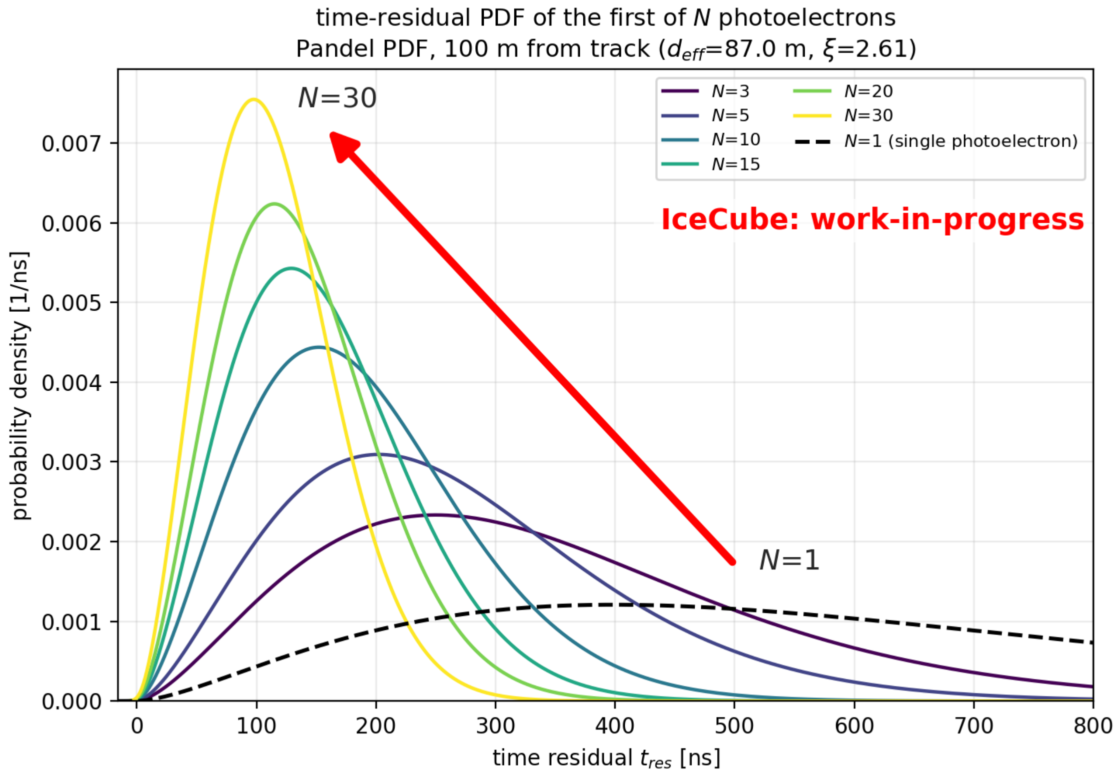

$$p_N^1(t_{\text{res}}) = N p_1(t_{\text{res}})[S_1(t_{\text{res}})]^{N-1}$$

- An inflated N pulls the PDF peak earlier and narrows it
- The fit then weights the wrong arrival times
- **→ the reconstructed direction can be biased**

Motivation: Limitations of the Current Afterpulse Model

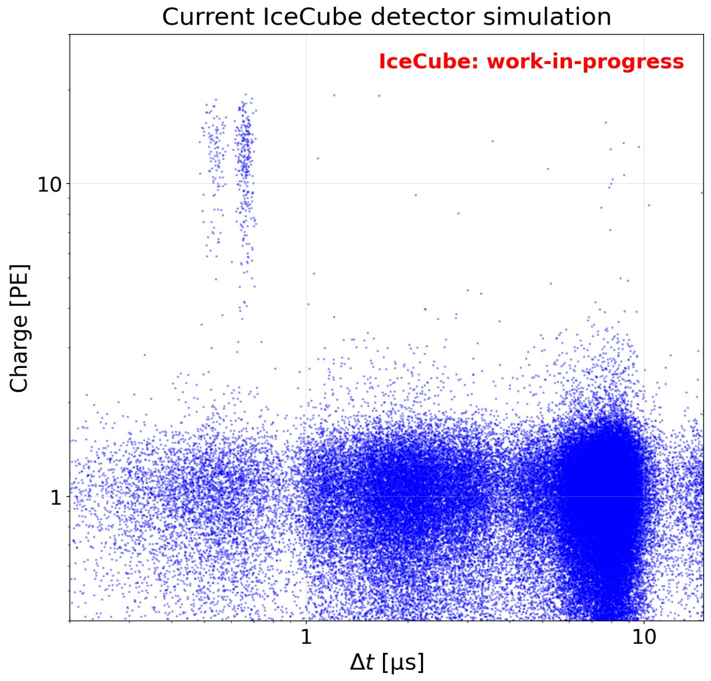

Ma et al., NIM A 629 (2011) 93–100.

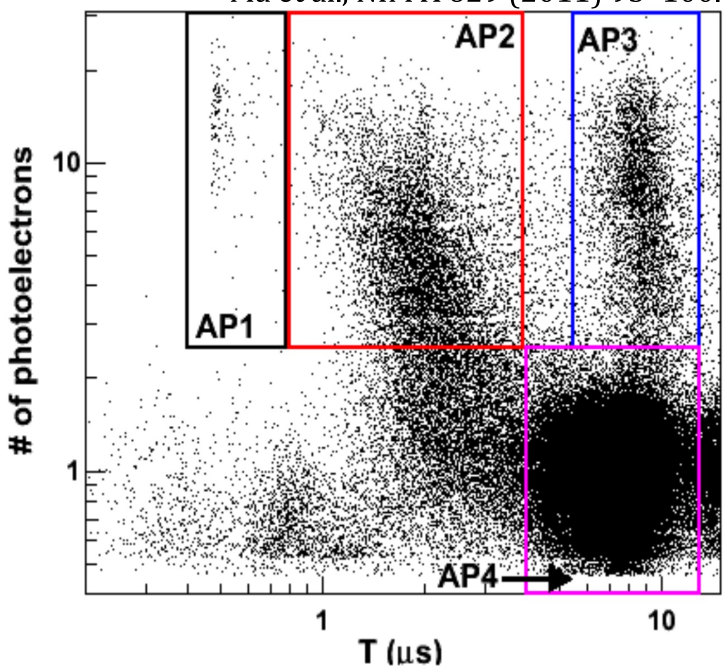

- The current simulation: a parametrization from laboratory measurements of a few PMTs (**left**)
- Time and charge are drawn independently (two 1D distributions)
- Ma et al. measured the joint distribution of the same PMT type: four groups, AP1 to AP4 (**right**)
- AP2 is time-charge correlated: independent 1D sampling cannot produce it
- Our goal: in-situ, detector-wide, time-charge characterization

This Work

- Dataset: in-situ IceCube data, 2011-2015 (5 seasons)
  - randomly sampled events with no physics selection: unbiased with respect to event type or brightness
  - full waveforms are recorded, spanning 6.4 μs per readout
  - every in-ice DOM reads out, so the sample covers the whole array
- Harvest: the delay and charge (Δt, Q) for every secondary pulse
  - main pulse: charge consistent with a single photoelectron (SPE)
  - from 7.0×10^9 readouts examined, 3.3×10^8 pulses over 5,058 DOMs
- Fit: a joint 2D model in (Δt, Q)
  - three afterpulse components following Ma et al., plus two backgrounds
  - one fit to the whole array first, giving the detector-averaged distribution

Selecting Afterpulse Candidates

- In-situ conditions: no dark box, no controlled source
  - muons, cascades and other in-ice light keep scattering into the afterpulse window
  - the main-pulse charge is measured, but its photoelectron content is not

Selecting Afterpulse Candidates

- In-situ conditions: no dark box, no controlled source
  - muons, cascades and other in-ice light keep scattering into the afterpulse window
  - the main-pulse charge is measured, but its photoelectron content is not
- Main pulse: [0, 50) ns from readout start, charge summed
  - a single photoelectron deposits 99.9% of its charge within 50 ns
- Main-pulse charge window: charge consistent with one photoelectron ($\pm 1\sigma$ around the single-PE charge peak)

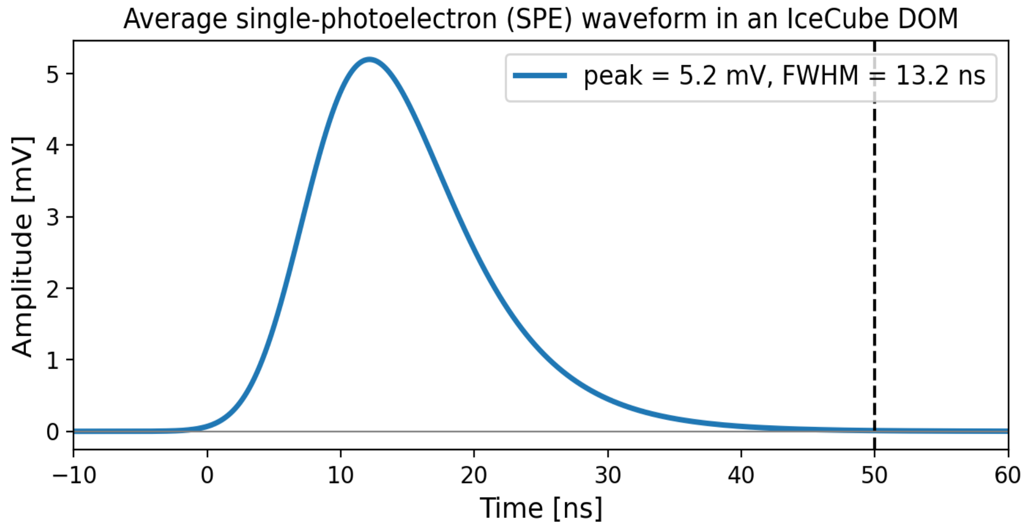

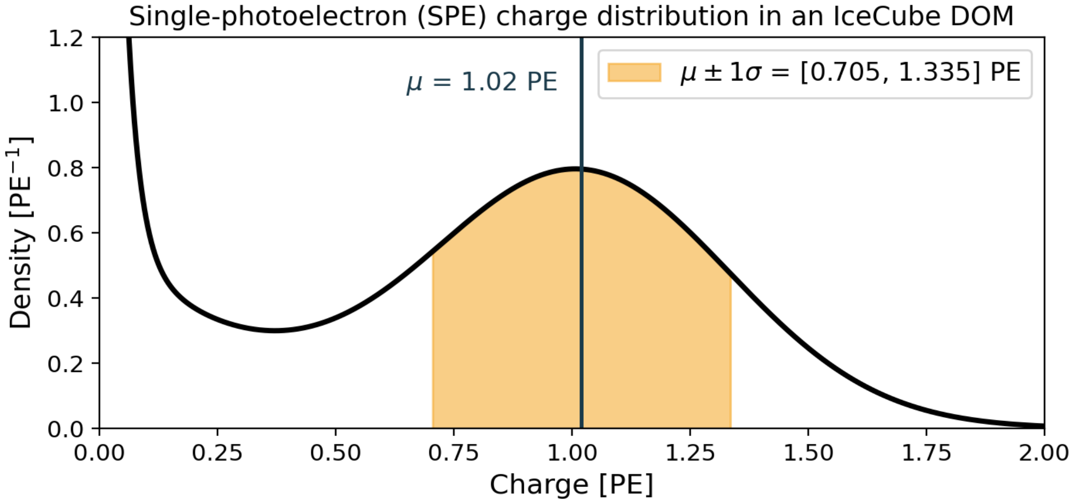

Parametrization from Abbasi et al. 2020, JINST 15 P06032

Selecting Afterpulse Candidates

- In-situ conditions: no dark box, no controlled source
  - muons, cascades and other in-ice light keep scattering into the afterpulse window
  - the main-pulse charge is measured, but its photoelectron content is not
- Main pulse: [0, 50) ns from readout start, charge summed
  - a single photoelectron deposits 99.9% of its charge within 50 ns
- Main-pulse charge window: charge consistent with one photoelectron ($\pm 1\sigma$ around the single-PE charge peak)
- No pulse in [50, 300) ns
  - a pulse there makes its own afterpulses, and late scattered light is still arriving

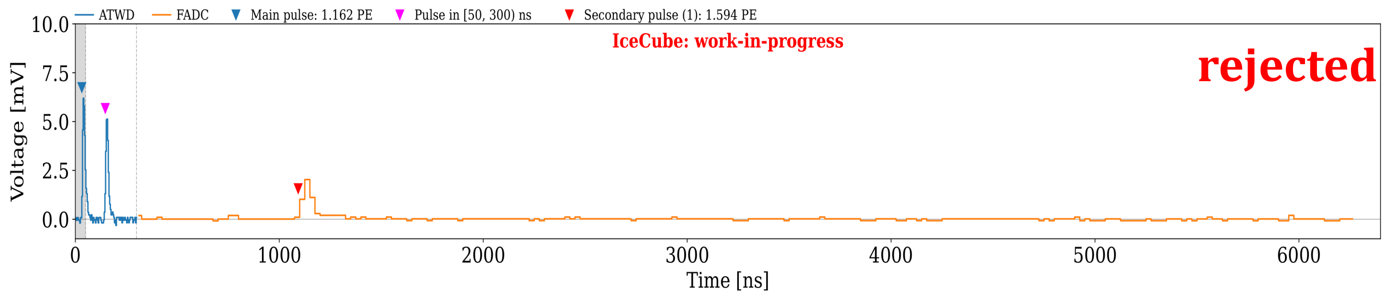

one pulse in [50, 300) ns
→ the secondary pulse cannot be assigned to the main pulse

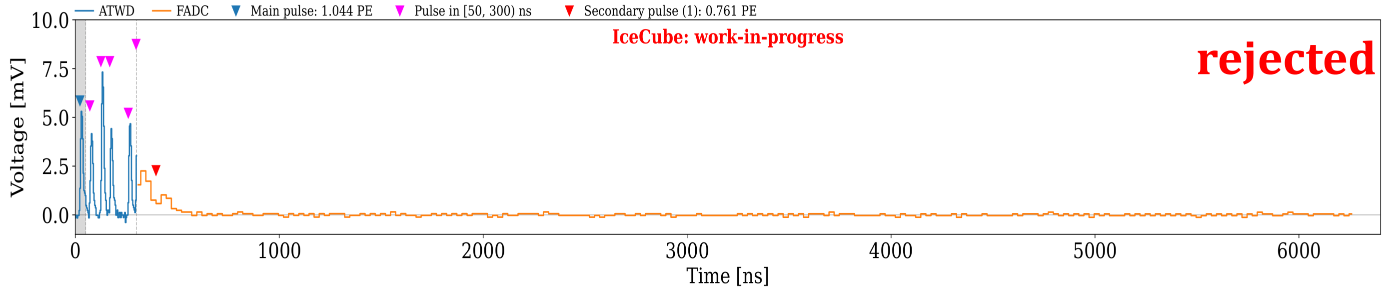

several pulses in [50, 300) ns
→ late scattered light is still arriving; pulses after 300 ns need not be afterpulses

Selecting Afterpulse Candidates

- In-situ conditions: no dark box, no controlled source
  - muons, cascades and other in-ice light keep scattering into the afterpulse window
  - the main-pulse charge is measured, but its photoelectron content is not
- Main pulse: [0, 50) ns from readout start, charge summed
  - a single photoelectron deposits 99.9% of its charge within 50 ns
- Main-pulse charge window: charge consistent with one photoelectron ($\pm 1\sigma$ around the single-PE charge peak)
- No pulse in [50, 300) ns
  - a pulse there makes its own afterpulses, and late scattered light is still arriving
- Afterpulse candidates: every secondary pulse with $\Delta t \in [0.3, 6.15]$ μs

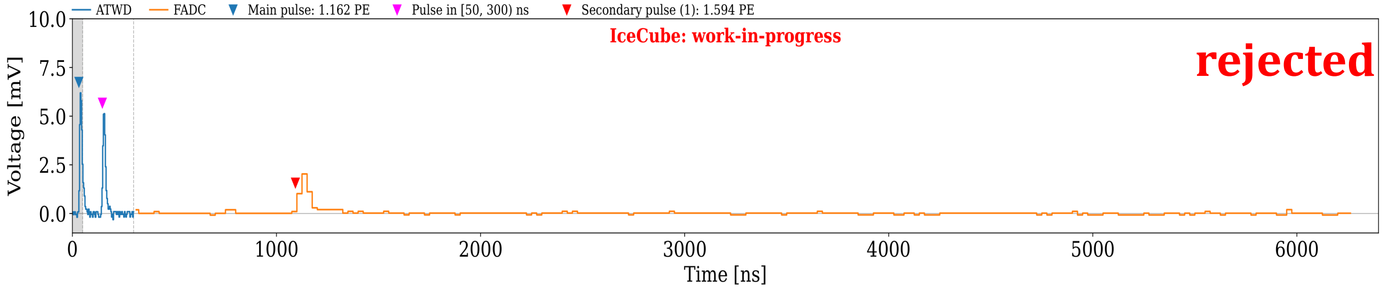

one pulse in [50, 300) ns
→ the secondary pulse cannot be assigned to the main pulse

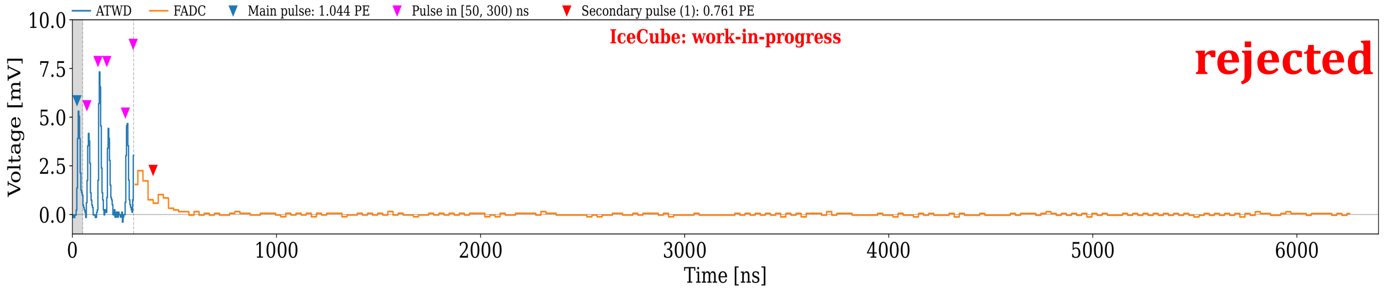

several pulses in [50, 300) ns
→ late scattered light is still arriving; pulses after 300 ns need not be afterpulses

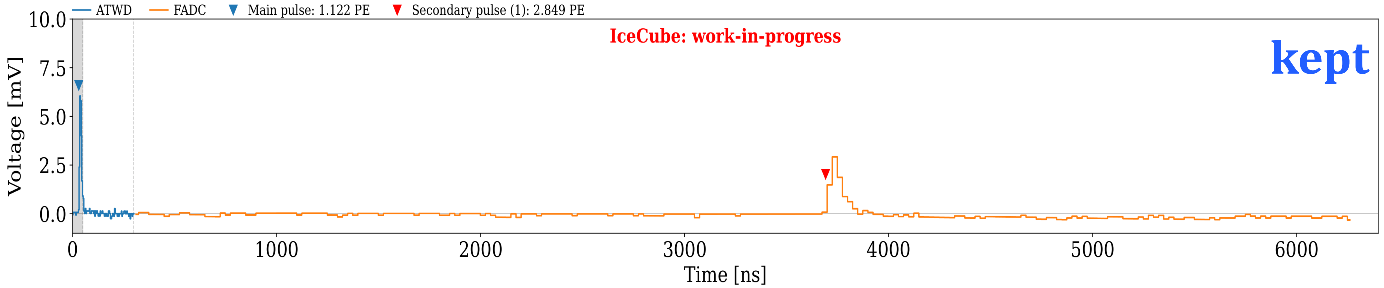

no pulse in [50, 300) ns
→ the secondary pulse can be assigned to the main pulse

Time-Charge Distribution

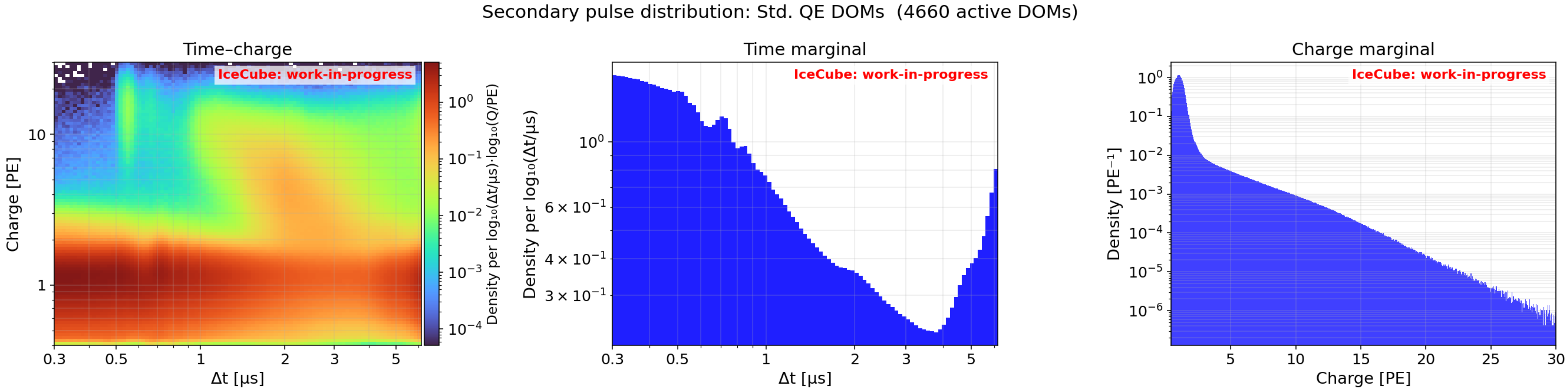

- In 2D, a broad low-charge component dominates, while two high-charge structures appear near 0.5 μs and 1-4 μs
- Time structure: sharp band near 0.5 μs, a falling tail down to ~4 μs, and the rise past 5 μs
- Charge marginal: SPE-dominated peak with a multi-PE tail across the full 30 PE range shown

Distribution Comparison

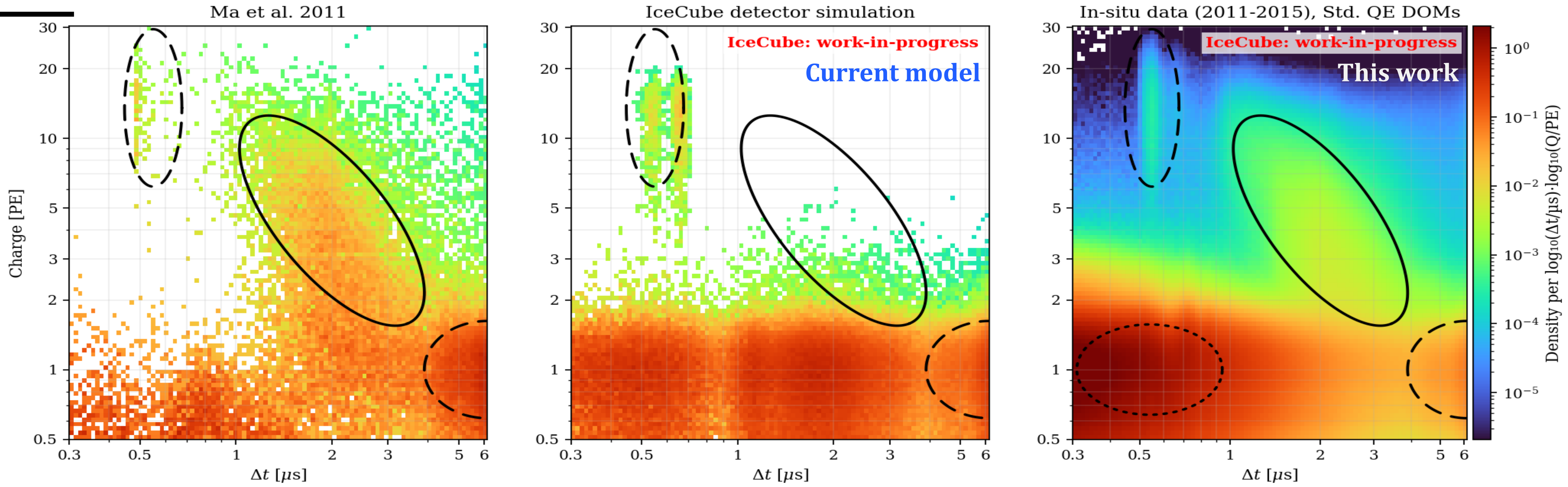

Simulation (middle): parametrization from lab measurements

- An early high-charge population (~0.5 μs) and a late SPE structure at the end of the window appear in **all** three samples **(dashed lines)**
- A time-charge correlated population (~1 to 4 μs) is present in Ma et al. and in the in-situ data, **absent** in simulation **(solid lines)**
- An early SPE excess ($\Delta t \lesssim 1$ μs) appears only in the in-situ data **(dotted line)**

Time-Charge Distribution Fit Model

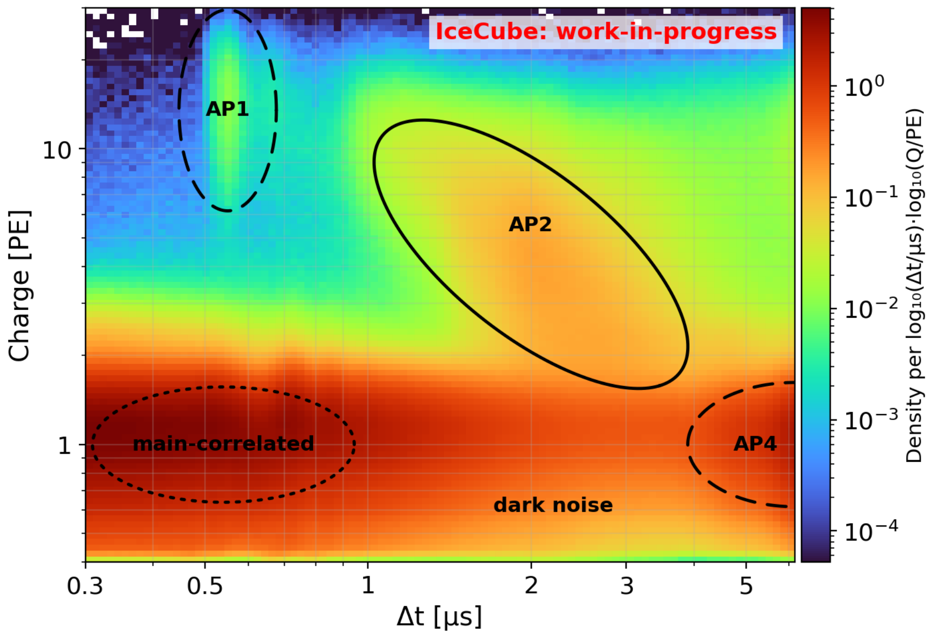

- Time-charge distribution fitting
  - Fitting space: $(x, y) = (\log_{10}(\Delta t/\mu s), \log_{10}(Q/PE))$
  - Fit window: $\Delta t \in [0.3, 6.15]$ μs, $Q \in [0.5, 30.5]$ PE
- Components and their models

component	time distribution model	charge distribution model
main-correlated	power law × exp cutoff (Pandel form)	compound Poisson
dark noise	uniform	SPE
AP1	bivariate Gaussian	
AP2	bivariate Gaussian	
AP4	Gaussian	SPE

Fitting Results: All DOMs

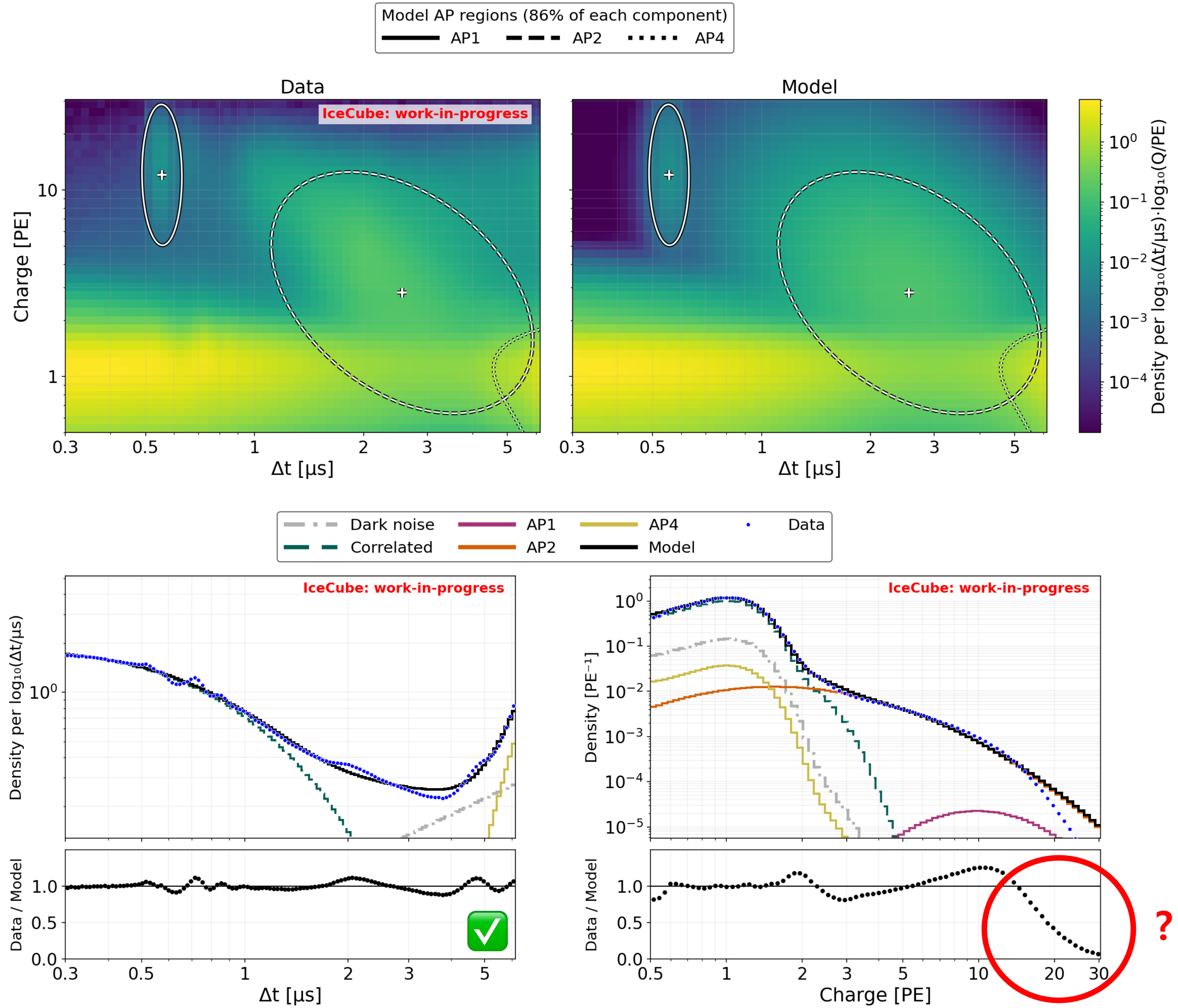

- The model reproduces the data in both time and charge
  - the model over-predicts the charge tail above ~15 PE
- AP2 carries most of the afterpulse charge

Limitations

- Main pulses are not a pure SPE sample, but the contamination is quantified
- Noise and coincident light cannot be separated from afterpulses
  - the separation is statistical, made by the joint fit
- The readout ends before the last afterpulse component (AP4) does
  - only its rising edge, past ~5 μs, falls inside the 6.15 μs fit window, so its position and width are only loosely constrained
- We cannot resolve which pulse caused which inside the window
  - an afterpulse can produce its own, so a late pulse may follow the main pulse or an earlier afterpulse
- The afterpulse rate is not extracted here; this measurement gives the shape of the distribution
  - the observed count depends on secondary-pulse detection and on the charge-dependent main-pulse selection
  - the remaining piece is the rate, so that shape and normalization both come from data

Summary

- From five years of in-situ IceCube data (2011-2015), we selected main pulses consistent with a single photoelectron on every in-ice DOM and harvested every pulse that followed within 0.3 to 6.15 μs; 3.3×10^8 pulses across 5,058 DOMs
- In ice, the joint (Δt, Q) distribution shows the components Ma et al. measured in the laboratory that fall inside our 6.15 μs window, including a high-charge population at 1 to 4 μs that the simulation, drawing time and charge independently, cannot produce
- The observed components can be explained by different ion species bombarding the photocathode, as in laboratory studies (Ma et al. 2011, Haser et al. 2013)
  - a complete matching of components to ion species has not been established and remains an open question
- A five-component fit reproduces the distribution in both time and charge, with a remaining over-prediction of the charge tail above about 15 PE that is still under study
- Next steps: put the in-situ model into the detector simulation to test the reconstruction and the noise rejection, and extract the afterpulse rate in situ
  - a better afterpulse model **could improve the modeling of the angular uncertainty**, and with it, the searches for astrophysical sources

Backup

Data Harvest – Main Pulse Window

- Main pulse
  - window: [0, 50) ns from readout start, charge summed
- Why 50 ns
  - The SPE template deposits 99.9% of its charge within 50 ns (99% by ~36 ns)
  - The readout is triggered by the main pulse itself, so it sits at the start of the window
- Why sum
  - wavedeform can split a single physical SPE into several pulses; summing can restore the SPE charge

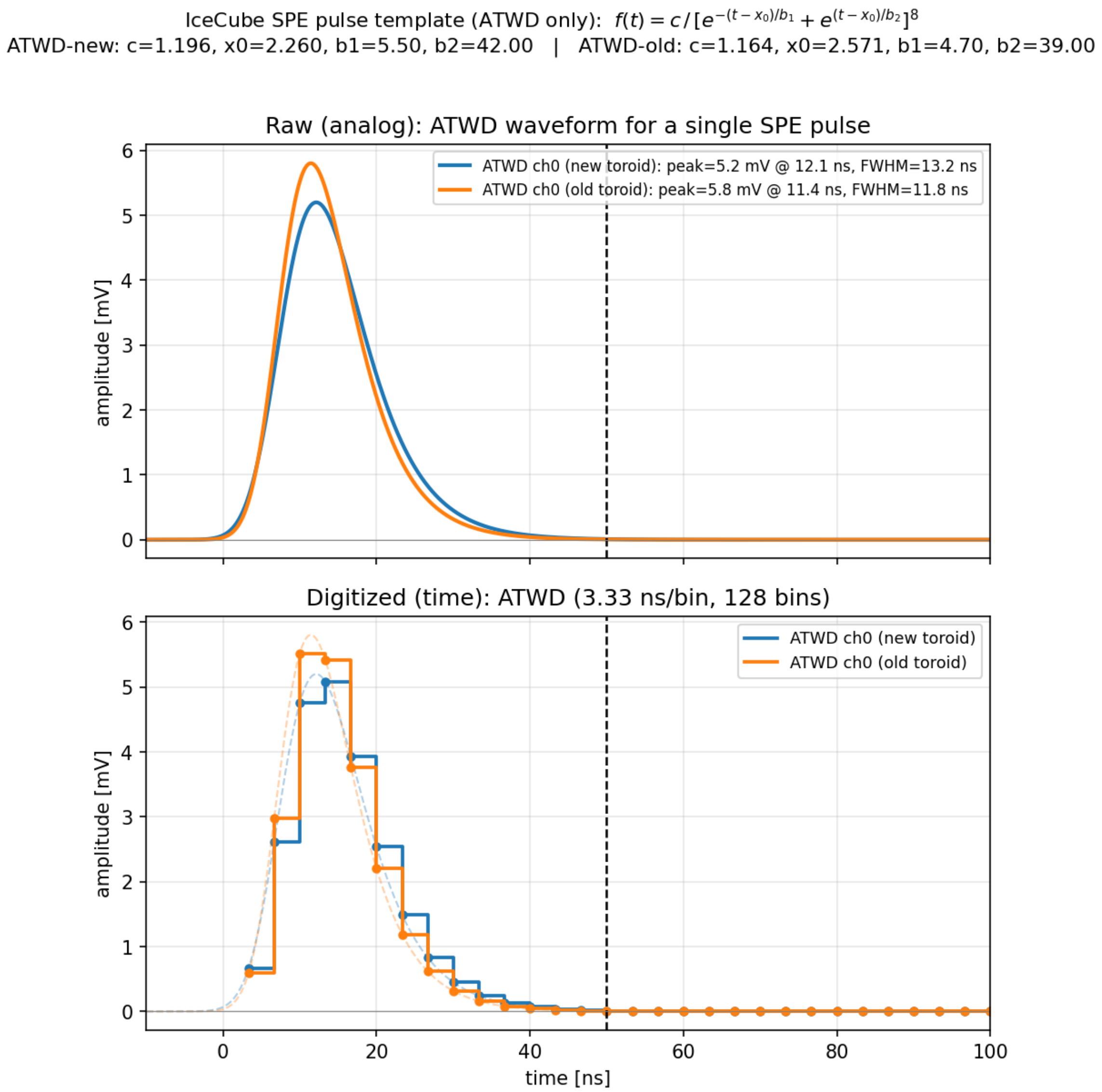

Data Harvest – Charge Cannot Count Photoelectrons

- A single photoelectron does not give a single charge
  - amplification is stochastic: the SPE charge PDF spans from ~0 to above 1 PE
- Readouts with 2, 3, … PEs cover the same charge range
  - no charge cut can separate them
- So the measured charge does not determine the number of PEs
  - a charge cut reduces the mixture but cannot remove it

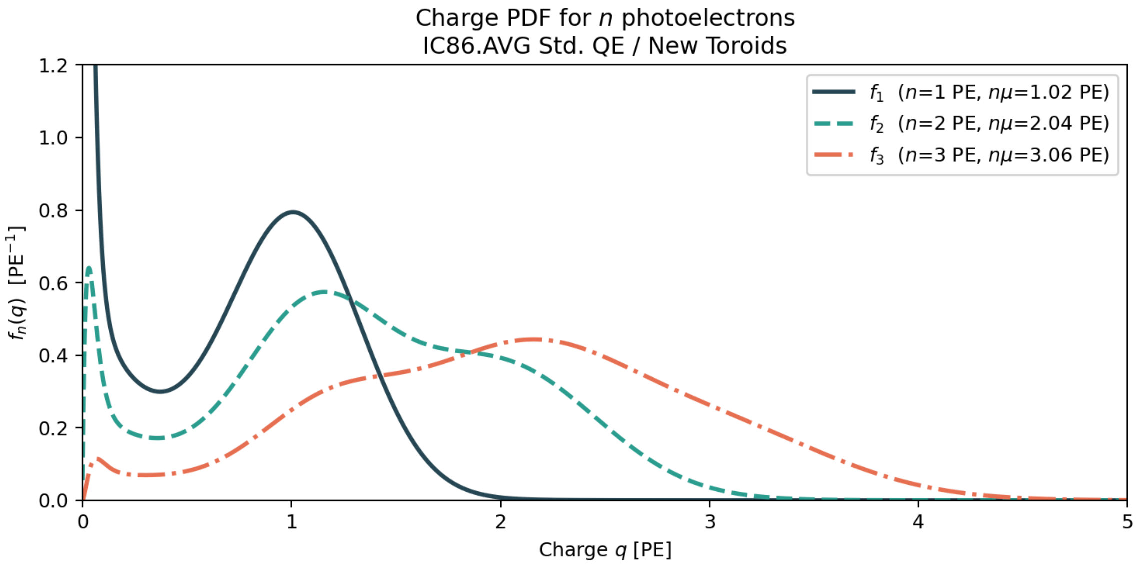

f_1: SPE charge template, eq. (2.1) and Table 1 of Abbasi et al. 2020, JINST 15 P06032
f_n: n-fold self-convolution of f_1, each normalized to 1 — the multi-PE model used there (§3.3), after Dossi et al., Nucl. Instrum. Meth. A 451 (2000) 623

Data Harvest – [50, 300) ns Constraint

- The constraint was introduced to keep Δt attributable, but it also sharpens the main-pulse selection
  - pass rate falls with main charge: ~78% at 1 PE, ~50% at 2 PE, ~ 17% at 5 PE
  - brighter launches leave more activity in [50, 300) ns

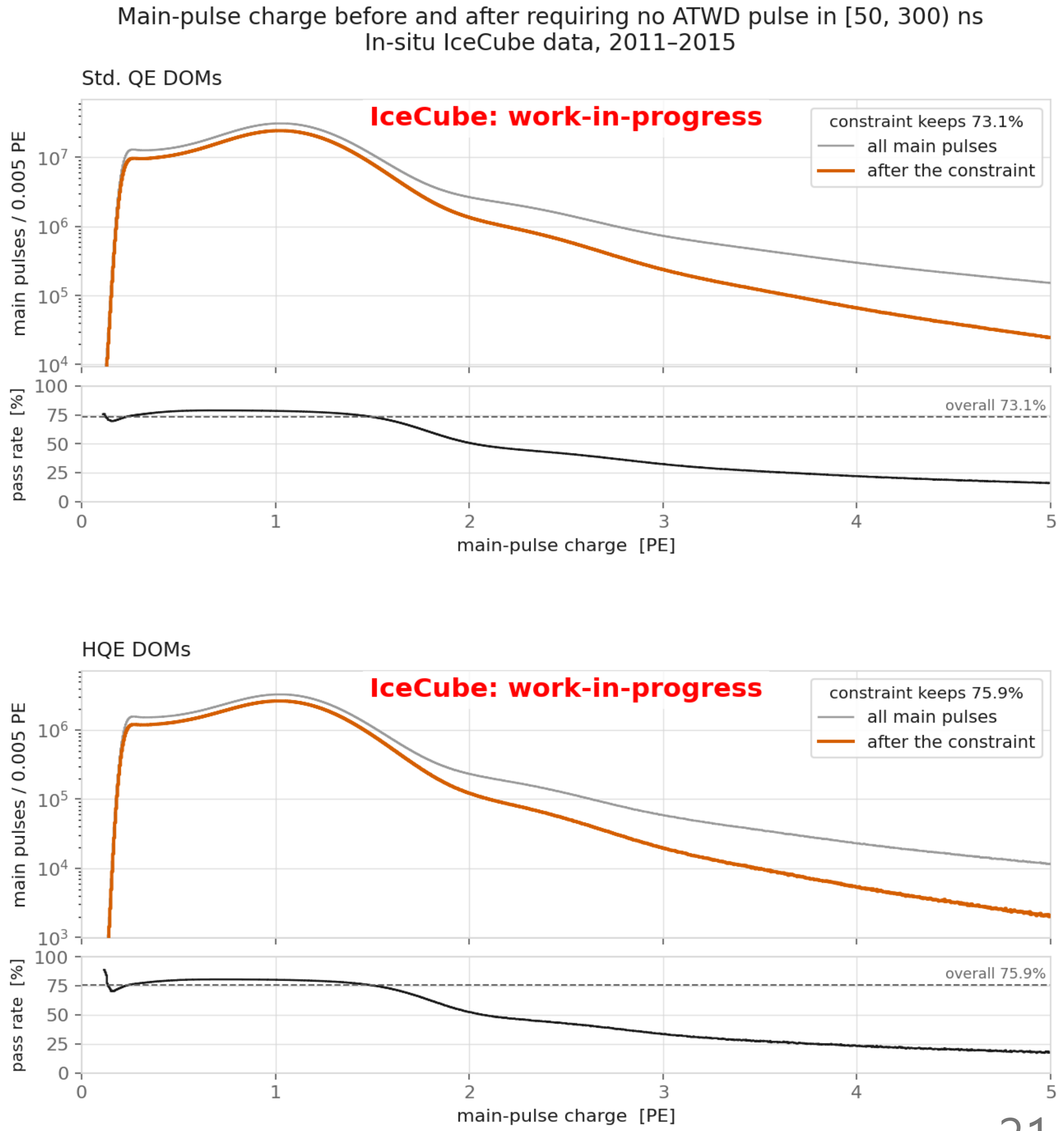

Data Harvest – Main-Pulse Charge Window

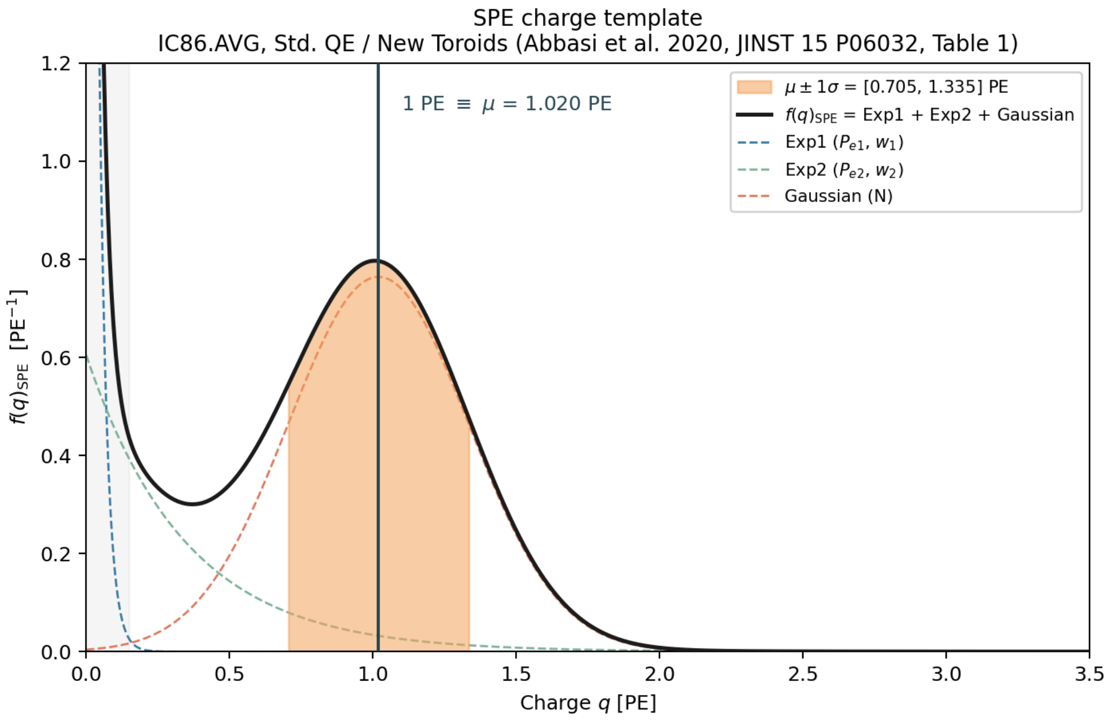

P_{e1}=0.186, w_1=0.027 PE; P_{e2}=0.211, w_2=0.348 PE; μ=1.0198 PE, σ=0.315 PE, N=1−P_{e1} − P_{e2}=0.603

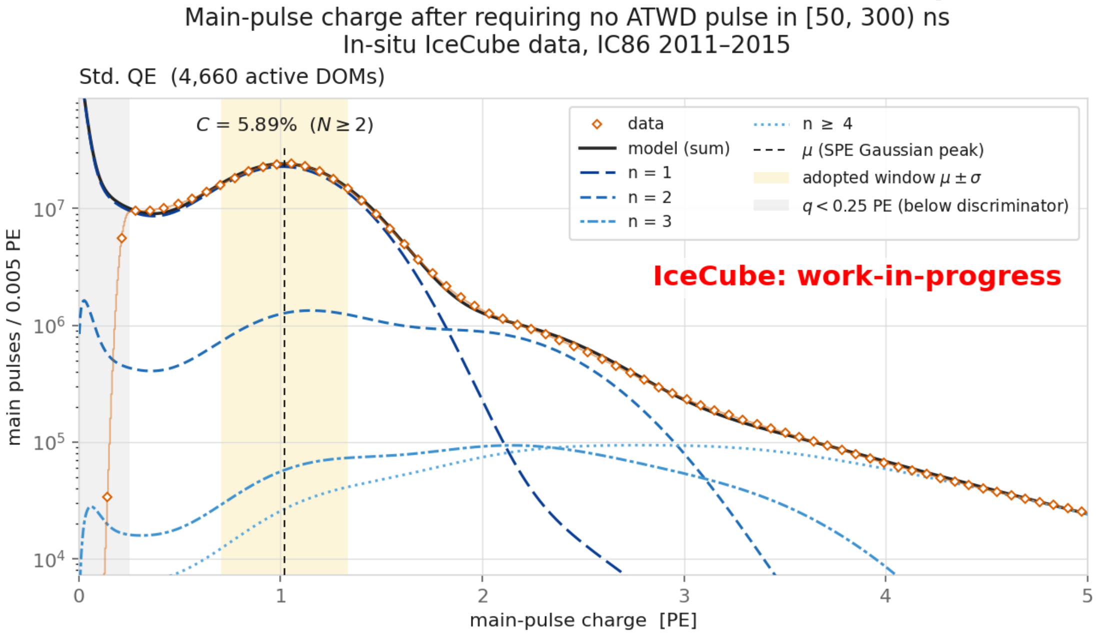

Single-PE template held fixed to Abbasi et al. 2020, JINST 15 P06032 Table 1 (Exp1 common to both subsets: P_{e1}=0.186, w_1=0.027 PE); only the multiplicity weights π_n ($n \leq 30$) are fitted, over 0.25–15.0 PE.
Std. QE DOMs: μ=1.0198 PE, σ=0.315 PE, P_{e2}=0.211, w_2=0.348 PE; $r = \pi_2/\pi_1$=0.0806, $N \geq 2$ contamination C=5.89%

- Window: $\mu \pm 1\sigma$ of the SPE Gaussian
  - 1 PE ≡ the Gaussian mean μ of the SPE template
  - window $\mu \pm 1\sigma$:
    - [0.705, 1.335] PE (Std. QE), [0.705, 1.327] (HQE)
- No charge window can remove N≥2, so we measured what is left
  - $C \approx 6\%$ (Std. QE), 4% (HQE)

window [PE]	statistics	N≥2 contamination
[0.99, 1.01] (previous)	1.0×	5.50%
$\mu \pm 0.5\sigma$	14.9×	5.68%
$\mu \pm 1\sigma$ (adopted)	27.2×	5.89%

- Why not narrower? → 27× the statistics for +0.39 %p contamination

Data Harvest – Sample Statistics

- Cut flow (2011-2015 combined)

selection stage	main pulse removed	main pulse remaining	remaining
ATWD pulse in $t_{\mathrm{rel}} \in [0,50)$ ns	-	7,008,178,410	100%
after [50, 300) ns constraint	1,871,322,102	5,136,856,308	73.3%
after main-charge window	2,229,718,561	2,907,137,747	41.5%

- Per-season statistics

season	contributing DOMs	selected main pulses	secondary pulses ($\Delta t \in [0.3,6.15]$ μs)	sec./main
2011	5,053	554,691,003	62,516,567	0.1127
2012	5,049	548,903,404	62,381,488	0.1136
2013	5,053	598,283,215	67,842,755	0.1134
2014	5,051	608,927,102	69,099,920	0.1135
2015	5,051	596,333,023	67,550,334	0.1133
2011-2015	5,058	2,907,137,747	329,391,064	0.1133

  - 3.3×10^8 secondary pulses over 5,058 DOMs — about 65k per DOM, enough for a DOM-by-DOM fit

Time-Charge Distribution – HQE

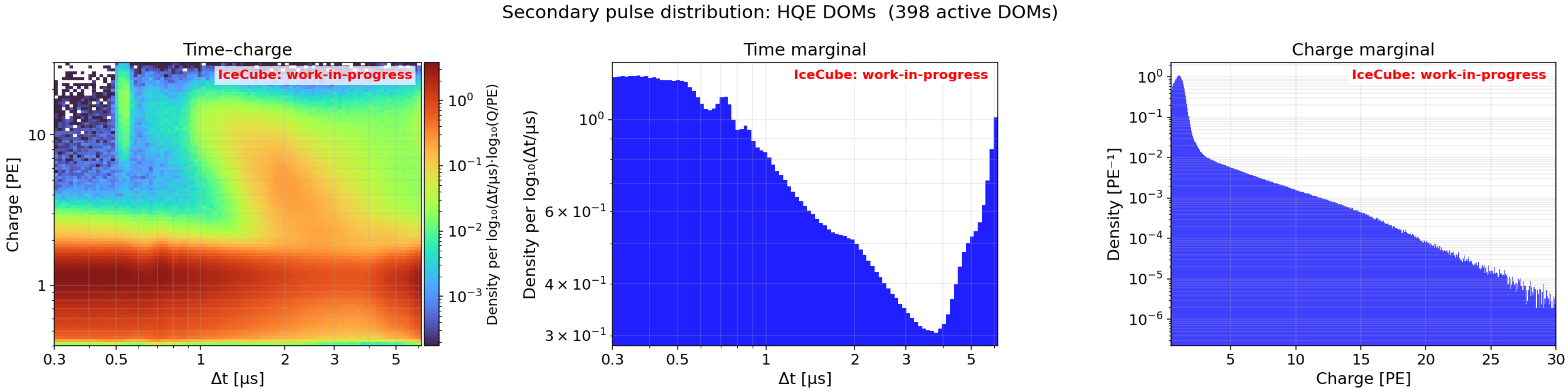

- Same time structure as Std. QE: sharp band near 0.5 μs, a falling tail down to ~4 μs, and the rise past 5 μs
- Charge marginal is also unchanged: SPE-dominated peak with a multi-PE tail
- Fewer HQE DOMs (~1/10 of Std. QE), so the statistics are lower, but no new structure appears
  - Expected: HQE and Std. QE share the same PMT structure, so the ion drift times that set the afterpulse timing are similar
  - → the same $(\Delta t, Q)$ model applies to both QE groups

Fitting Results: All DOMs (HQE)

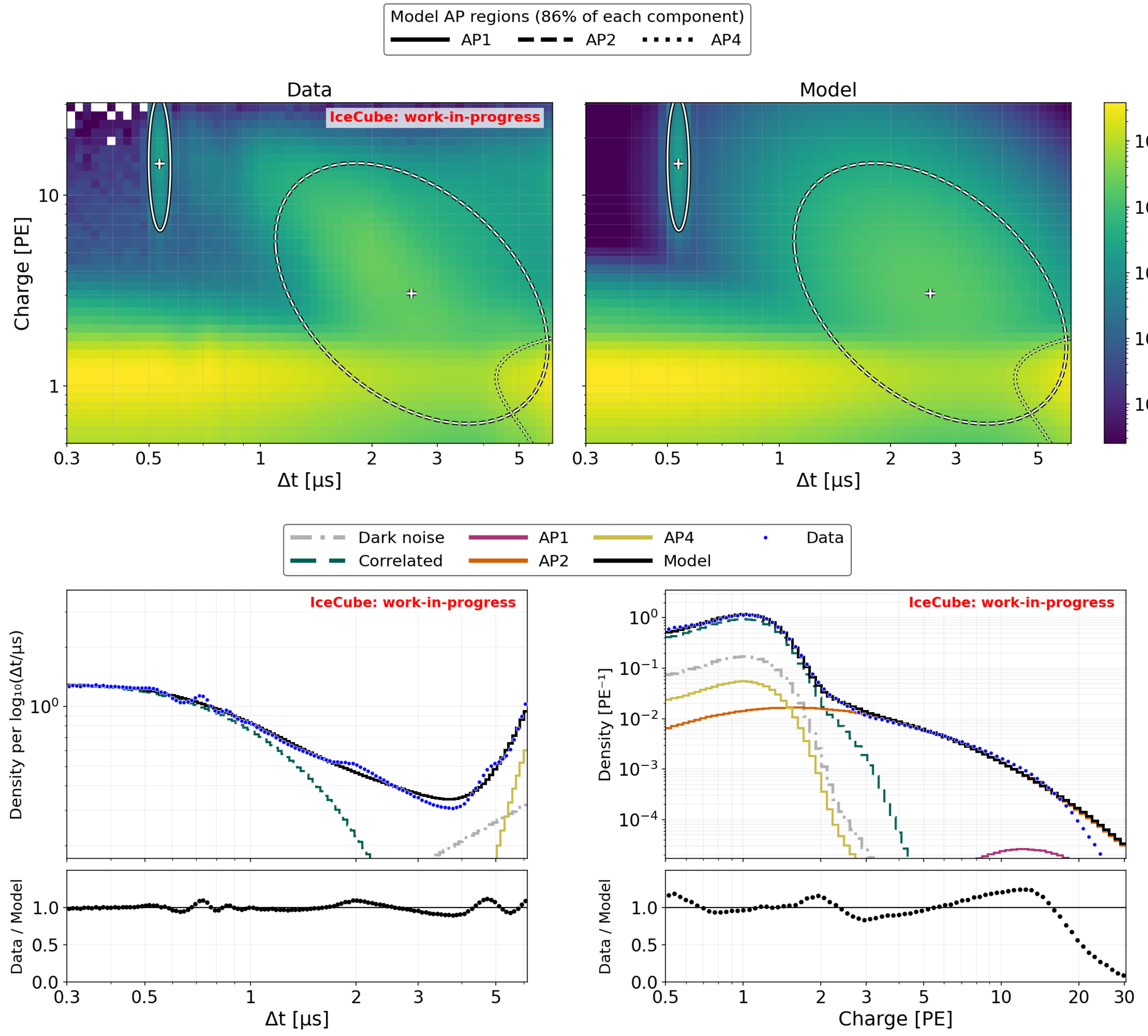

- The same five components also fit the HQE DOMs
  - the charge tail above ~15 PE is over-predicted the same way
- The shape of the afterpulse distribution is essentially unchanged